5-21-2017

2D Unsteady Routing and Flood Inundation Mapping for Lower Region of Brazos River Watershed

Manahari Bhandari
Southern Illinois University

Narayan Nyaupane
Southern Illinois University

Shekhar Raj Mote
Southern Illinois University

Ajay Kalra
Southern Illinois University, kalraa@siu.edu

Sajjad Ahmad
University of Nevada, Las Vegas, sajjad.ahmad@unlv.edu

2D Unsteady flow routing and flood inundation mapping for lower region of Brazos River watershed.

Manahari Bhandari[1], Narayan Nyaupane[1] Shekhar Raj Mote[1], Ajay Kalra[1] and Sajjad Ahmad[2]

[1]Department of Civil and Environmental Engineering, Southern Illinois University Carbondale, 1230 Lincoln Drive, Carbondale, IL 62901-6603.

[2]Department of Civil and Environmental Engineering and Construction, University of Nevada Las Vegas, 4505 S. Maryland Parkway, Las Vegas, NV 89154-4015.

Abstract

Present study uses two dimensional flow routing capabilities of Hydrologic Engineering Center's River Analysis System (HEC-RAS) for flood inundation mapping in lower region of Brazo River watershed subjected to frequent flooding. For analysis, river reach length of 20 km located at Richmond, Texas, was considered. Detailed underlying terrain information available from digital elevation model of 1/9-arc second resolution was used to generate the two-dimensional (2D) flow area and flow geometrics. Streamflow data available from gauging station USGS08114000 was used for the full unsteady flow hydraulic modeling along the reach. Developed hydraulic model was then calibrated based on the manning's roughness coefficient for the river reach by comparison with the downstream rating curve. Corresponding water surface elevation and velocity distribution obtained after 2D hydraulic simulation were used to determine the extent of flooding. For this, RAS mapper's capabilities of inundation mapping in HEC-RAS itself were used. Mapping of the flooded areas based on inflow hydrograph on each time step were done in RAS mapper, which provided the spatial distribution of flow. The results from this study can be used for flood management as well as for making land use and infrastructure development decisions..

Keywords: HEC-RAS, Flood Inundation, 2D flow, Unsteady flow

Introduction

Increase in global temperature since 1950 has been observed throughout the world. The main cause of this warming is the anthropogenic greenhouse gases (Field et al., 2014; Pokhrel et al., 2012). Warming has intensified the hydrologic cycle (Kalra and Ahmad, 2011,2012; Pathak et al., 2016a, b). The effect of climate change has been observed by various studies (Carrier et al., 2013, 2016). Different models and scenario have shown extreme flooding throughout the world (Ahmed and Tsanis, 2016; Keuler et al., 2016; Ranger et al., 2011; Tamaddun et al., 2016a, b). The rise in global temperature increases the risk of extreme flood (Milly et al., 2002; Sagarika et al., 2014). The warming causes increase in surface temperature of the water bodies. Increase in surface temperature enhances the evaporation and ultimately rainfall (Kalra et al., 2013 a,b; Sagarika et al., 2015a, b). This phenomenon impacts magnitude and frequency of the precipitation and eventually floods. In the urban landscapes, where the infiltration capacity of the landscape is

significantly reduced due to the construction of impervious structure and compaction of subsurface, the intensity and peak of discharge are significantly increased (Kalra et al. 2013c). As a result, the severity of flood in the downstream increases, leading to increased socio-economic and ecological destruction (Dawadi and Ahmad, 2012; Paz et al., 2013; Maheswari et al., 2014; Dhakal and Chevalier, 2016).

In situ flood observation is the best approach to analyze the flood risk (Hagen and Lu, 2011; Zhang et al., 2014, 2016). Flood hazard and flood risk mapping are the fundamental tools for flood management (Mosquera-Machado & Ahmad, 2007; Mostert and Junier, 2009; Ghimire et al., 2016). Flooding events occurring annually in various parts of the world has resulted in serious impact on humans and the economy. In the United States, where floods are the most common natural disaster, $4 billion per year in average was claimed for total flood insurance between 2003 and 2012 (NFIP, 2016). Predicting the extent and occurrence of flood events has always been a challenge to the parties involved in managing flood (Ahmad and Simonovic, 2006). Delineation of floodplains is the requirement of National Flood Insurance Act which was established by Congress in 1968 (FEMA, 2016). Based on which, National Flood Insurance Program (NFIP) has been stablished. With the frequent occurrence of extreme events in urban areas, flood models and floodplain maps have become necessary (Knebl et al., 2005; Forsee and Ahmad, 2011).

Various hydraulic models are used to simulate the flooding events to support the decision-making process regarding the prediction and prevention of floods (Ahmad and Simonovic, 2006; Thakali et al., 2016;). Various studies have shown capability of commercially available version of 2D numerical simulation models (Seyoum et al., 2012; Sanders, 2007; Quiroga et al., 2013). Performance of traditional 1D models is questionable in very flat floodpains. Thus, many 1D hydraulic models are being replaced by 2D hydraulic models (Merwade et al. 2008). Though there is huge uncertainty about the characteristics of flood event, two-dimensional numerical analysis offers a way to better characterize the flood. HEC-RAS hydraulic model has been widely used in conjunction with Environmental System Research Institute (ESRI) ArcGIS software and HEC-GeoRAS for 1D analysis and mapping of floods. The latest version, HEC-RAS 5.0.1 offers the stand-alone capability to perform 2D hydraulic routing and capabilities of detailed animation and mapping of flood within the RAS mapper in HEC-RAS itself. This ability allows hydraulic engineers to analyze model results through the geospatial visualization to more readily identify hydraulic model deficiencies and make model improvements (Engineers 2002).

This paper explores the 2D modeling capacity of HEC-RAS to model the Brazos river reach in Richmond, Texas area, which is subjected to frequent flooding. The latest abilities of RAS mapper in HEC-RAS are exploited for the enhanced mapping of the floodplain in the region by using the historical flow data of the river. The objective of study is to perform the unsteady flow analysis and prepare a flood plain map of the study area to outline the flood prone areas by using the 2D hydraulic modeling and mapping capabilities of latest version of HEC-RAS.

Study Area and Data

Richmond, Texas lies on the floodplain of the Brazos River. The flat plain area of the Richmond is vulnerable to the flooding in Brazos. The study floodplain has centroidal coordinate of 29°35’N

and 95°45’W. The considered reach length of the river is almost 20 km and the river along this reach is meandering in shape. The reason for selecting this study area was the frequent flooding events occurring in this area impacting a dense urban population around it. The Brazos River has many reservoirs and tributaries with frequent changes in flow rate and water level. Thus, timely information to those residing near surface water in the Brazos basin, and around the Richmond area in this study is vital.

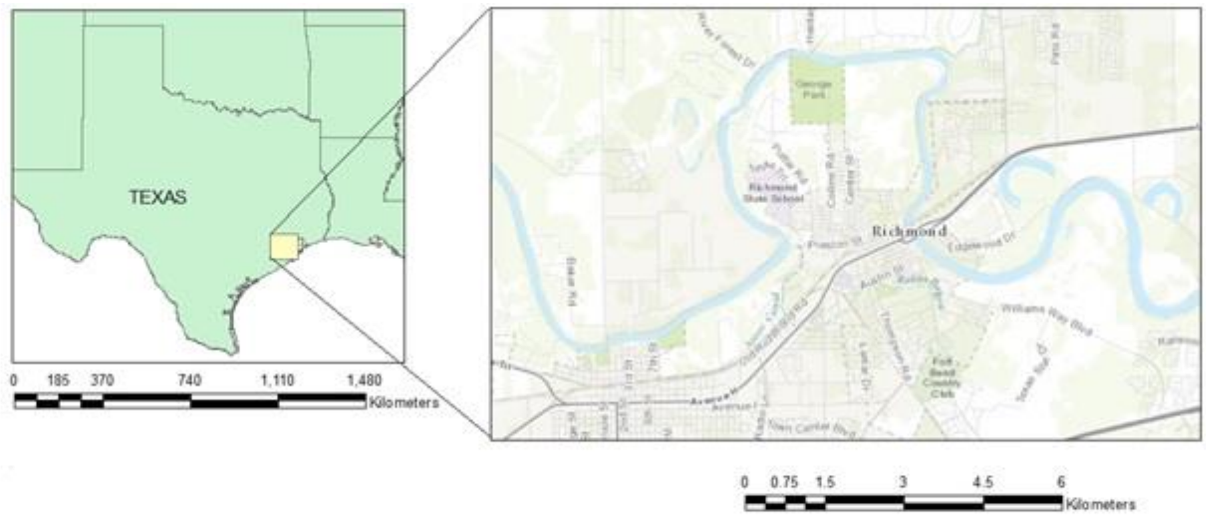

Figure 1: Study area (Richmond, Texas on the bank of Brazos river)

1/9 arc second Digital Elevation Model (DEM) was used for creating terrain of the study area in RAS mapper, which was obtained from United States Geological Survey (USGS)- The National Map Viewer website. For the simulation of HEC-RAS hydraulic model, streamflow data from USGS gage station 08114000 was used. Land cover data for providing the manning’s roughness coefficient for river channel and bank was obtained from National Land Cover Database (NLCD).

Methodology

Available DEM data was imported in HEC-RAS to create the terrain model in RAS-Mapper which was then used for establishing the geometry and hydraulic properties of 2D flow area. Cells of dimension 3mX3m were created along the 2D flow area of the river reach. Hydraulic properties of each cell were then created by running geometric pre-processor in RAS Mapper.

NLCD 2011 dataset was used in GIS to create the land cover grid with the associated manning’s roughness coefficient (n) which was assigned within the 2D flow areas. The assigned land cover value and corresponding manning’s n value are shown in Table 1.

Upstream (U/S) and Downstream (D/S) boundary condition lines were created to provide the boundary condition values for unsteady flow simulation. In the U/S, USGS gauging station stream hydrograph was used for the analysis, whereas for D/S boundary condition normal depth channel slope (0.0007) was used. Developed geometric layer with the used boundary condition is shown in**Error! Reference source not found.** figure 2(a).

Table 1: Manning's n value for the area

Value	Description	Manning's n value
11	Open Water	0.035
21	Developed, Open Space	0.0404
22	Developed, Low Intensity	0.0678
23	Developed, Medium Intensity	0.0678
24	Developed, High Intensity	0.0404
31	Barren Land (Rock/Sand/Clay)	0.0113
41	Deciduous Forest	0.36
42	Evergreen Forest	0.32
43	Mixed Forest	0.4
52	Shrub/Scrub	0.4
71	Grassland/Herbaceous	0.368
81	Pasture/Hay	0.325
82	Cultivated Crops	0.3228
90	Woody Wetland	0.086
95	Emergent Herbaceous Wetlands	0.1825

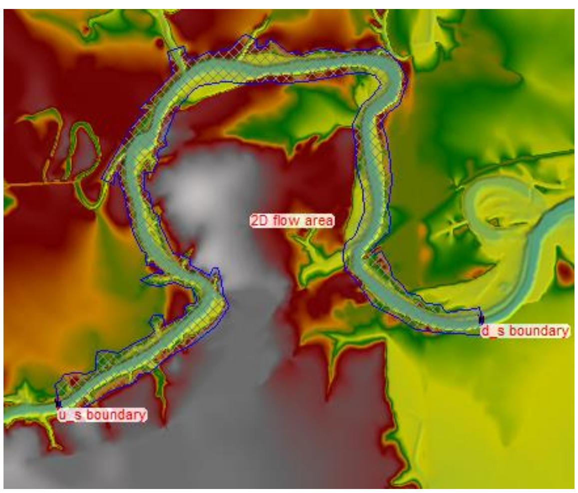

(a)

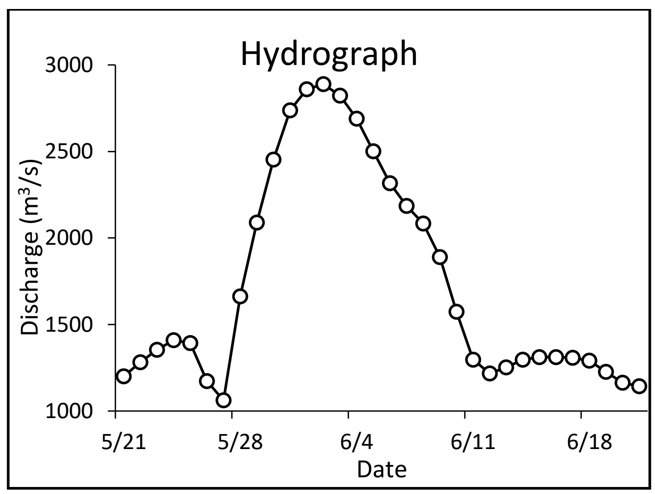

(b)

Figure 2: Geometric data with computed cell meshing (a) & input hydrograph for HEC-RAS model (b).

For the unsteady flow simulation, daily discharge data for the periods of 21st May 2016-21st June 2016 was used. Over the period, maximum river flow occurred on June 2nd 2016 with discharge value of 2888 m^3/s. Hydrograph used in analysis is shown in Figure 2(b)**Error! Reference source not found.**. The rating curve at D/S gauging station was used. Calibration of the model was done by altering the manning's roughness value of the river channel within the previously provided land cover grid.

Flood inundation mapping for the maximum flow in the river was plotted in RAS mapper. Additional map layers of google earth imagery can also be added in the RAS mapper for the enhanced visualization.

The flow chart of the methodology is shown in the Figure 3.

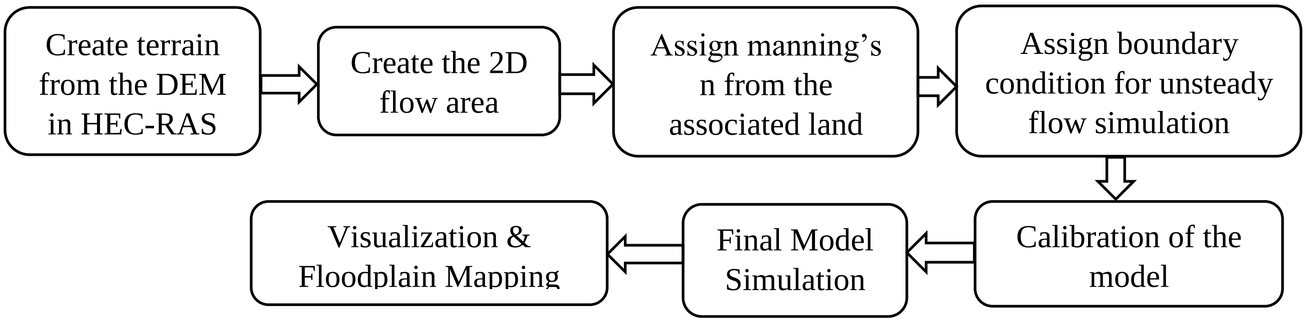

Figure 3: Stepwise methodology involved for HEC-RAS analysis and floodplain mapping

Results and Discussions

Imported terrain data was used for creating the 2D flow area within geometry editor and total number of 536381 cells were created over the 2D river flow area within the river reach length of 20 KM. Each cell size 3m*3m was used for the analysis with the computational time interval of 10 min with the output interval of 1 day. Small time interval and small cell size selection is better for getting good result though the simulation takes more time to complete. For the unsteady flow analysis in HEC-RAS, initial conditions of river were assumed to be wet even though default mode of HEC-RAS simulation is dry. Assuming this condition, at first HEC-RAS will fill up the mesh till the warmup time and then simulation will be done with that filled cells of river as open channel flow using diffusion wave equation considering the finite volume approximation.

Before doing analysis in HEC-RAS, hydraulic properties of each cell should be assigned. HEC-RAS has capability of creating hydraulic properties of each computed cell mesh. Those hydraulic properties are based on the provided geometric terrain data as well as provided manning's n value land cover grid. Representation of assigned cell properties are shown in Figure 4. The number 62 is the represented cell number and manning's n value taken for that cell is 0.325. Figure also shows linear volume-elevation and volume-wetter perimeter relationships for that cell.

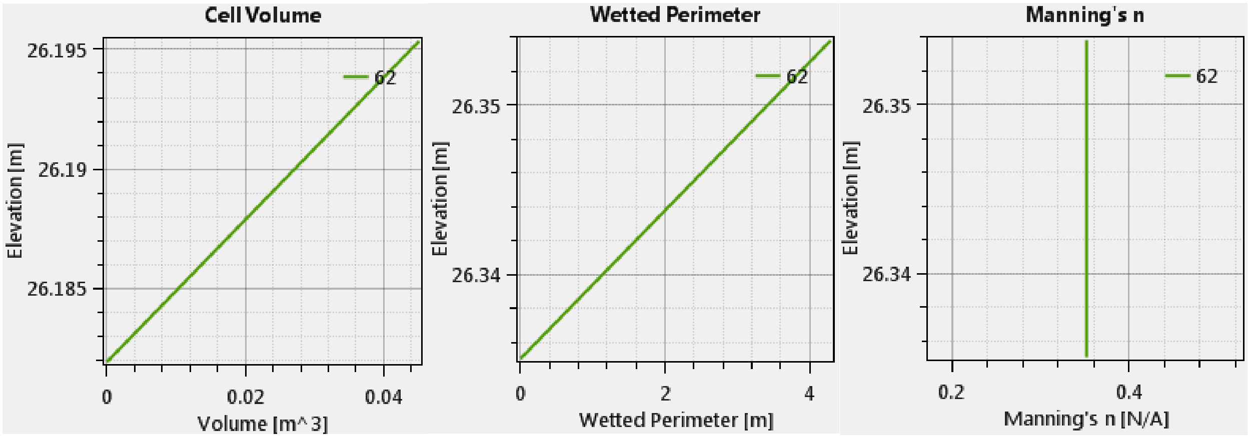

(a) (b) (c)

Figure 4: Representation of hydraulic properties created within HEC-RAS. Elevation vs. volume (a), Elevation vs. wetted perimeter (b) & elevation vs. manning's coefficient (c).

Calibration of the model was done by comparing the simulated water surface elevation value of river with the observed water surface elevation from the gauging station 08114000 for the period of 5/22/2016-6/21/2016 shown in Figure 5 (a) & (b). From the observed and simulated data, correlation coefficient (r) was found to be 0.997 and coefficient of determination (R^2) was found to be 0.995 shown in Figure 5 (c). From the analysis, the correlation between observed and simulated data found to be satisfactory.

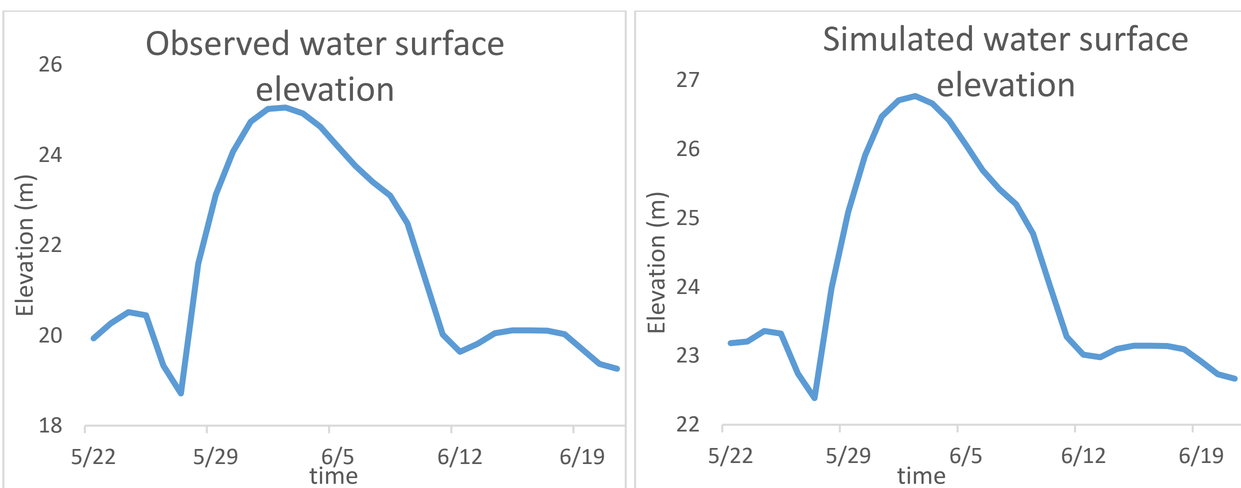

(a) (b)

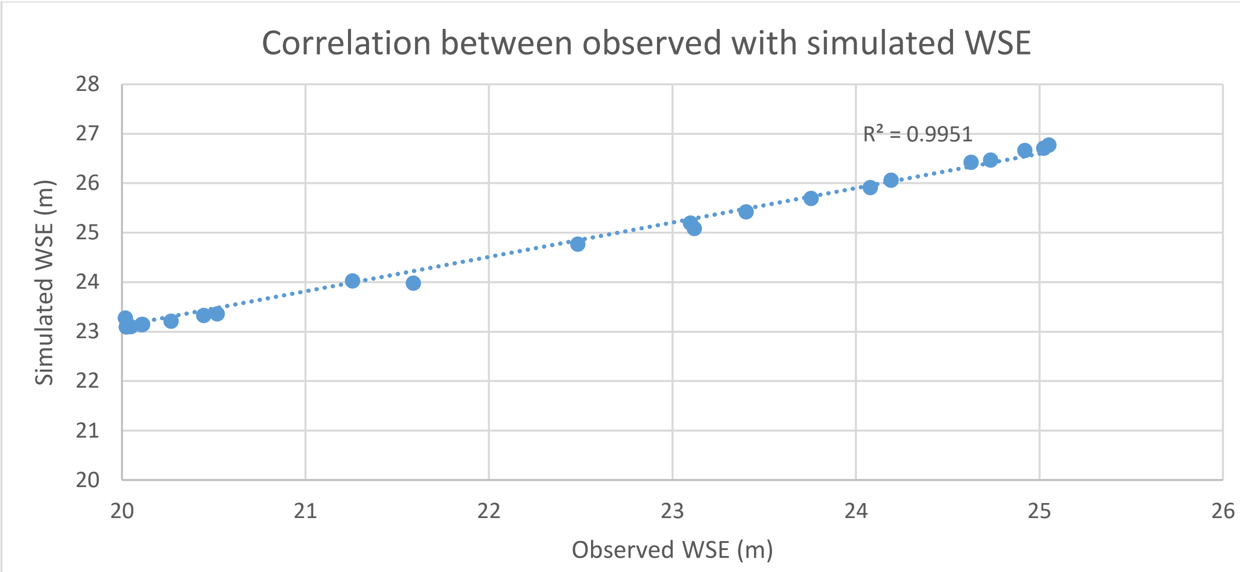

(c)

Figure 5: Observed & simulated water surface elevation (a) & (b). Correlation between observed and simulated water surface elevation (c).

From the HEC-RAS analysis, the time variation of result of unsteady flow analysis was obtained. The water depth, water velocity and water surface elevation within the time series is found to be maximum when there was maximum flow, though, the location of maximum value of each result got varied over the reach with time. The location is dependent upon the cell properties and associated geometry.

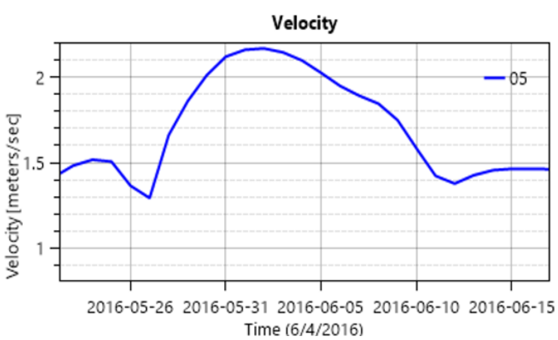

(a)

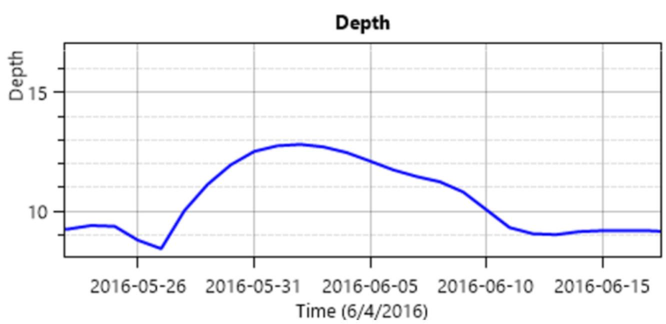

(b)

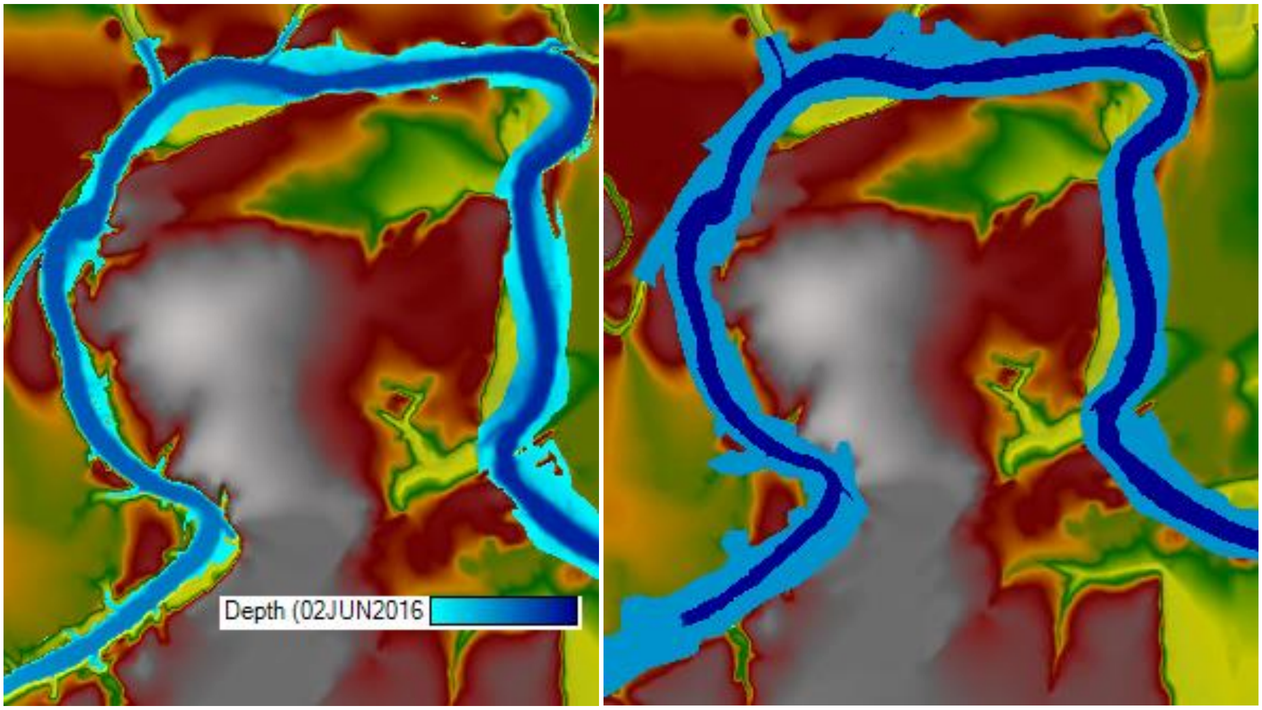

(c) (d)

Figure 6: Velocity & depth ditribution with respect to time at gauging station location (a) & (b). Water depth distribution for maximum flow (c) & percentage area inundated more than 7m (d).

Velocity distribution of the river at gauging station location is shown in the Figure 6(a)**Error! Reference source not found.**. Maximum velocity of 2.2 was observed at that location. The depth distribution for that station is also plotted in Figure 6(b). Maximum depth obtained was 12.8 m. For the entire river reach, the maximum velocity of 16.1 m/s occurred at 505.2 m downstream of starting location.

The maximum Water depth distribution for the maximum flow value of 2888 m^3/s which occurred on June 2^{nd} 2016 was plotted in RAS mapper as shown in Figure 6 (c). Maximum water depth of 13.1m was obtained over the reach at location of 1334 m downstream from the starting location. This result is the representation of flooding occurred for the year 2016.

Percentage flood inundation graph was also generated for the river reach. The threshold depth of 7 m is chosen. In RAS mapper, within the 2D flow area, the % of time the flood has reached the depth above 7m on each cell is potted as shown in Figure 6(d). The result with darker blue color represent maximum percentage of time the flow depth occurred more than 7 m within the 2D flow area. Figure represents almost all flow area has been inundated above 7 m depth. During the flooding event (2^{nd} June), the water surface reached up to 26.8 m depth inundating the entire flow area considered.

Conclusion

This study was aimed to conduct 2D unsteady flow simulation using HEC-RAS 5.01 in Brazos river watershed. For the river of 20 km reach length, flow hydrograph for period of 21^{st} may 2016-

21st June 2016 consisting of a flooding event was routed. Using the available geometric data and land cover data associated with manning's roughness coefficient, calibration of flow simulation with measured water surface elevation was done. Evaluation of unsteady flow situation for the whole month as well as flooding event was carried out. From the analysis following conclusions can be drawn.

- During the analysis period, the maximum water depth obtained was 13.1 m and maximum flood velocity was 16.1 m/s, which is at the time of peak runoff at the location mentioned above. The results obtained were found to be related with hydraulic properties of cells as well as cell size and geometry of terrain.
- When peak flow of 2888 m^3/s was routed entire flow area was found to be inundated. The maximum water surface elevation reached was 26.8 m. The result resembled with the flooding that happened on 2nd June 2016 in the Richmond area.
- The extent of flooding would certainly increase if the discharge in the river soars, which is likely to happen due to the climate change.

2D unsteady flow analysis is hence found to be suitable to depict the time series result for the given flow condition. Animation capabilities provided in HEC-RAS gives the clear understanding with visual result. Particle tracing observation also gives relative flow velocity and flow direction based on the distance and direction moved by particle during the simulation. It is seen from the model output that the flow level has changed as per the discharge value. The result suggested that maximum velocity and depth distribution is associated with the flooding event. Further, HEC-RAS simulation also depends upon the warmup time provided and computation interval. Small computational interval and small cell size gives good result but takes time to complete the full unsteady analysis.

However, the flooding around the Richmond area that has been evident in the past years is not fully explained by this floodplain mapping as it is related only to stream discharge of particular month. The peak urban runoff might also be the reason behind such unexpected flooding, which needs further research for its validation. Some discrepancies between observed water surface elevations and simulated flow may be attributed to course DEM data. Although the flood hazard management strategy of the Richmond, TX has not been discussed here, similar analysis of the Brazos River may help the areas for demarcating safe and vulnerable zones based on the extent of the flood. Such analysis also can be used for the prediction of flood hazard as well as its extent and can be useful for the timely evacuation during the flooding events. Capabilities of HEC-RAS for 2D analysis could be a good tool for flood management.

Reference

Ahmad, S., & Simonovic, S. P. (2006). "An intelligent decision support system for management of floods." *Water Resources Management,* 20(3), 391-410.

Ahmed, S. and Tsanis, I. (2016). "Climate Change Impact on Design Storm and Performance of Urban Storm-Water Management System-A Case Study on West Central Mountain Drainage Area in Canada." *Hydrology: Current Research 2016.*

Carrier, C., Kalra, A., & Ahmad, S. (2013). “Using Paleo Reconstructions to Improve Streamflow Forecast Lead Time in the Western United States.” *Journal of the American Water Resources Association*, 49(6), 1351–1366. doi:10.1111/jawr.12088.

Carrier, C. A., Kalra, A., & Ahmad, S. (2016). “Long-range precipitation forecasts using paleoclimate reconstructions in the western United States.” *Journal of Mountain Science,* 13(4), 614-632.

Dawadi, S., & Ahmad, S. (2012). “Changing climatic conditions in the Colorado River Basin: implications for water resources management.” *Journal of Hydrology,* 430, 127-141.

Dhakal, K.P., Chevalier, L.R. (2016). "Urban Stormwater Governance: The Need for a Paradigm Shift." *Environmental Management 57(5),* 1112-1124. doi:10.1007/s00267-016-0667-5

Diodato, N., Bellocchi, G., Romano, N. and Chirico, G.B. (2011). "How the aggressiveness of rainfalls in the Mediterranean lands is enhanced by climate change." *Climatic Change 108(3),* 591-599.

Engineers, U.A.C.O. (2002) HEC RAS River Analysis System. Hydraulic Reference Manual.

FEMA (2016) Federal Emergency Management Agency

Field, C.B., Barros, V.R., Dokken, D.J., Mach, K.J., Mastrandrea, M.D., Bilir, T.E., Chatterjee, M., Ebi, K.L., Estrada, Y.O., Genova, R.C., Girma, B., Kissel, E.S., Levy, A.N., MacCracken, S., Mastrandrea, P.R. and White, L.L. (eds), "Climate Change 2014: Impacts, Adaptation, and Vulnerability. Part A: Global and Sectoral Aspects. Contribution of Working Group II to the Fifth Assessment Report of the Intergovernmental Panel on Climate Change (IPCC) (2014)." *Cambridge University Press, Cambridge, United Kingdom, and New York, NY, USA.* pp.1-32

Forsee, W. J., & Ahmad, S. (2011). Evaluating urban storm-water infrastructure design in response to projected climate change. *Journal of Hydrologic Engineering, 16(11),* 865-873.

Ghimire, G. R., Thakali, R., Kalra, A., & Ahmad, S. (2016). "Role of Low Impact Development in the Attenuation of Flood Flows in Urban Areas." In *World Environmental and Water Resources Congress 2016* (pp. 339-349).

Hagen, E. and Lu, X. (2011). "Let us create flood hazard maps for developing countries." *Natural hazards 58(3),* 841-843.

Kalra, A., & Ahmad, S. (2011). “Evaluating changes and estimating seasonal precipitation for the Colorado River Basin using a stochastic nonparametric disaggregation technique.” *Water Resources. 47,* W05555. http://dx.doi.org/10.1029/ 2010WR009118.

Kalra, A., & Ahmad, S. (2012). “Estimating annual precipitation for the Colorado River Basin using oceanic-atmospheric oscillations.” *Water Resources Research*, 48(6), W06527. doi:10.1029/2011WR010667.

Kalra, A., Li, L., Li, X., & Ahmad, S. (2013a). “Improving streamflow forecast lead time using oceanic-atmospheric oscillations for Kaidu river basin, Xinjiang, china.” *J. Hydrological Eng. 18 (8),* 1031–1040.

Kalra, A., Miller, W. P., Lamb, K. W., Ahmad, S., & Piechota, T. (2013b). “Using large-scale climatic patterns for improving long lead time streamflow forecasts for Gunnison and San Juan River Basins.” *Hydrological Processes, 27(11),* 1543–1559. doi:10.1002/hyp.9236.

Kalra, A., Ahmad, S., & Nayak, A. (2013c). “Increasing streamflow forecast lead time for snowmelt-driven catchment based on large-scale climate patterns.” *Advances in Water Resources,* 53, 150–162. doi:10.1016/j.advwatres.2012.11.003.

Keuler, K., Radtke, K., Kotlarski, S. and Lüthi, D. (2016). "Regional climate change over Europe in COSMO-CLM: Influence of emission scenario and driving global model." *Meteorologische Zeitschrift*, 121-136.

Knebl, M., Yang, Z.-L., Hutchison, K. and Maidment, D. (2005). "Regional scale flood modeling using NEXRAD rainfall, GIS, and HEC-HMS/RAS: a case study for the San Antonio River Basin Summer 2002 storm event." *Journal of Environmental Management 75(4)*, 325-336.

Maheshwari, P., Khaddar, R., Kachroo, P., & Paz, A. (2014). "Dynamic Modeling of Performance Indices for Planning of Sustainable Transportation Systems." *Networks and Spatial Economics*, 1-23.

Merwade, V., Cook, A. and Coonrod, J. (2008). "GIS techniques for creating river terrain models for hydrodynamic modeling and flood inundation mapping." *Environmental Modelling & Software 23(10)*, 1300-1311.

Milly, P.C.D., Wetherald, R.T., Dunne, K. and Delworth, T.L. (2002). "Increasing risk of great floods in a changing climate." *Nature 415(6871)*, 514-517.

Mosquera-Machado, S., & Ahmad, S. (2007). "Flood hazard assessment of Atrato River in Colombia." *Water Resources Management, 21(3)*, 591-609.

Mostert, E. and Junier, S. (2009). "The European flood risk directive: challenges for research." *Hydrology and Earth System Sciences Discussions 6(4)*, 4961-4988.

NFIP (2016) National Flood Insurance Program. *https://www.fema.gov/national-flood-insurance-program*

Pathak, P., Kalra, A., & Ahmad, S. (2016a) "Temperature and precipitation changes in the Midwestern United States: implications for water management." *International Journal of Water Resources Development*, 1-17. http://doi.org/10.1080/07900627.2016.1238343.

Pathak, P., Kalra, A., Ahmad, S., & Bernardez, M. (2016b). "Wavelet-aided analysis to estimate seasonal variability and dominant periodicities in temperature, precipitation, and streamflow in the Midwestern United States." *Water Resources Management*, 30(13), 4649-4665. http://doi.org/10.1007/s11269-016-1445-0

Paz, A., P. Maheshwari, P. Kachroo, & S. Ahmad (2013). "Estimation of performance indices for the planning of sustainable transportation systems." *Advances in Fuzzy Systems*, 2.

Pokhrel, Y. N., Hanasaki, N., Yeh, P. J. F., Yamada, T. J., Kanae, S., & Oki, T. (2012). "Model estimates of sea level change due to anthropogenic impacts on terrestrial water storage" *Nat. Geosci.*, 5, 389–392.

Quiroga, V.M., Popescu, I., Solomatine, D. and Bociort, L. (2013). "Cloud and cluster computing in uncertainty analysis of integrated flood models." *Journal of Hydroinformatics 15(1)*, 55-70.

Ranger, N., Hallegatte, S., Bhattacharya, S., Bachu, M., Priya, S., Dhore, K., Rafique, F., Mathur, P., Naville, N. and Henriet, F. (2011). "An assessment of the potential impact of climate change on flood risk in Mumbai." *Climatic Change 104(1)*, 139-167.

Sagarika, S., Kalra, A., & Ahmad, S. (2014). "Evaluating the effect of persistence on long-term trends and analyzing step changes in streamflows of the continental United States." *Journal of Hydrology*, 517, 36-53. doi:10.1016/j.jhydrol.2014.05.002.

Sagarika, S., Kalra, A., Ahmad, S. (2015a). "Interconnection between oceanic-atmospheric indices and variability in the US streamflow." *Journal of Hydrology 525, 724–736. doi:10. 1016/j.jhydrol.2015.04.020.*

Sagarika, S., Kalra, A., Ahmad, S. (2015b). "Pacific Ocean and SST and Z500 climate variability and western U.S. seasonal streamflow." *International Journal of Climatology 36,* 1515–1533. doi:10.1002/joc.4442

Sanders, B.F. (2007). "Evaluation of on-line DEMs for flood inundation modeling." *Advances in Water Resources 30(8),* 1831-1843.

Seyoum, S.D., Vojinovic, Z., Price, R.K. and Weesakul, S. (2012). "Coupled 1D and Noninertia 2D Flood Inundation Model for Simulation of Urban Flooding." *Journal of Hydraulic Engineering* 138(1), 23-34.

Tamaddun, K. A., Kalra, A., Ahmad, S. (2016a). "Wavelet analysis of western U.S. streamflow with ENSO and PDO." *Journal of Water and Climate Change,* 1–15. http://doi.org/10.2166/wcc.2016.162.

Tamaddun, K., Kalra, A., Ahmad, S. (2016b). "Identification of Streamflow Changes across the Continental United States Using Variable Record Lengths." *Hydrology, 3(2),* 24. http://doi.org/10.3390/hydrology3020024.

Thakali, R., Kalra, A. and Ahmad, S. (2016). "Understanding the Effects of Climate Change on Urban Stormwater Infrastructures in the Las Vegas Valley." *Hydrology 3(4),* 34. doi:10.3390/hydrology3040034

Zhang, F. Y., Li, L. H., Ahmad, S., & Li, X. M. (2014). "Using path analysis to identify the influence of climatic factors on spring peak flow dominated by snowmelt in an alpine watershed." *Journal of Mountain Science*, 11(4), 990-1000.

Zhang, F., Ahmad, S., Zhang, H., Zhao, X., Feng, X., & Li, L. (2016). "Simulating low and high streamflow driven by snowmelt in an insufficiently gauged alpine basin." *Stochastic Environmental Research and Risk Assessment*, 30(1), 59-75.